

Disorder induced lifetime effects in binary disordered systems : a first principles formalism and an application to doped Graphene

Banasree Sadhukhan[†], Subhadeep Bandyopadhyay[‡], Abhijit Mookerjee^{*1}

^{1†} *Department of Physics, Presidency University,
86/1 College Street, Kolkata 700073, India.*

[‡] *Department of Physics, Presidency University, 86/1 College Street, Kolkata 700073, India*

[‡] *Department of Solid State Physics, Indian Association for the Cultivation of Science,
2A-2B, Raja Subodh Kumar Mullick Road, Jadavpur. Kolkata 700032, India
S.N. Bose National Centre for Basic Sciences, JD-III, Salt Lake, Kolkata 700098, India.*

(Dated: June 18, 2019)

In this work the conducting properties of graphene lattice having particular concentration of defect has been studied. Here we have used the real space block recursion method introduced by Haydock et al. Here the defects are completely random. This Green function based method is more powerful than the usual reciprocal based methods which need artificial periodicity. Also we don't need to solve the Schrödinger equation to solve for the wave functions. Different resonant states appear because of the presence of topological and local defects are studied within the framework of Green function.

I. INTRODUCTION

In 1928 Felix Bloch¹ introduced to the solid state community his famous theorem which immediately started an avalanche of activity on the band structure of electrons in crystalline solids. It gave scientists a very useful handle to solve the electronic part of the differential equation (later formally derived by Kohn and Sham^{2,3}. Bloch's ideas were applications to solid state physics of the earlier works of three mathematicians : George William Hill⁵ (1827), Gaston Floquet⁴ (1883) and Alexander Lyapunov⁸ (1928). Bloch^{1,6,7} argued that for a second order linear differential equation

$$\mathcal{D}(\vec{r})\Psi(\vec{r}) = E\Psi(\vec{r}),$$

then, provided the differential operator satisfies lattice translation symmetry : $\mathcal{D}(\vec{r}) = \mathcal{D}(\vec{r} + \vec{\chi})$, there exists a *real* vector \vec{k} , such that the solution is :

$$\Psi_{\vec{k}}(\vec{r}, E) = \exp\{i\vec{k} \cdot \vec{r}\}u_{\vec{k}}(\vec{r}, E)$$

Note that the vector \vec{k} is necessarily *real* and labels both the quantum state and its energy. Bloch applied it to the Kohn-Sham equation for a crystalline solid, where

$$\mathcal{D}(\vec{r}) = -(1/2)\nabla^2 + V(\vec{r}) \quad \text{with } V(\vec{r}) = V(\vec{r} + \vec{\chi})$$

The rush to join the Bloch bandwagon was so great that many uncomfortable questions that rose from time to time with the Bloch theorem being violated were systematically swept under the carpet. From the seminal work by Andersen⁹, Chandrasekhar^{10,11} and Mott¹² it became clear that disorder which violates Bloch Theorem can give rise to new phenomena where disorder cannot be regarded as a small perturbation on a crystalline background.

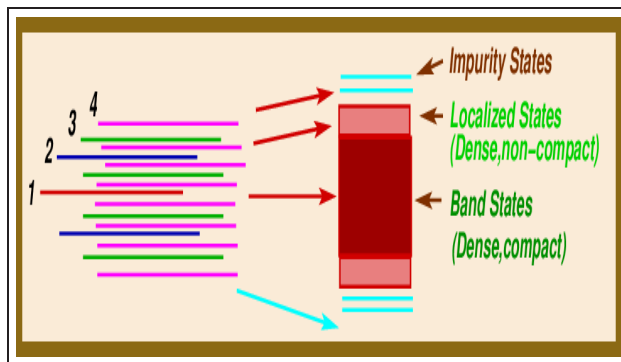


Figure 1: (Colour online) Anderson's picture of evolution of bands from discrete spectrum of finite systems.

In particular, the picture proposed by Anderson and illustrated in Fig. 1, is worth review. In a finite system, say an atom or a molecule, the spectrum is discrete labelled by discrete quantum labels $\{n\}$. As the size of the molecule increases the number of discrete eigenvalues also increase. Moreover, if $\{E_n^{(L)}\}$ is the set of eigenvalues of a molecule of size L , then the eigenvalues of the system of size L exactly *nest* those of size $L-1$. If, as $L \rightarrow \infty$ the spectrum of the solid is bounded, then by Cantor's Theorem, the asymptotic spectrum \mathcal{S} consists of two parts : \mathcal{S}_1 in which the spectrum remains discrete. This part describes impurities, bound states and does not exist in pristine systems. \mathcal{S}_2 , which is a dense, compact set and represents the electron bands in a pristine solid.

$$E_{n-1}^{(L-1)} \leq E_n^{(L)} \leq E_n^{(L-1)}$$

For disordered system, there is a third type of spectrum \mathcal{S}_3 which is dense but not compact. This part represents the Anderson localized states.

Thus, the problem arises, in case the premises of Bloch Theorem breaks down, how do we proceed to study such disordered solids further.

II. THE SUPERCELL TECHNIQUE.

A large section of physicists, ever reluctant to let go of the Bloch crutch, turned to ‘supercell’ techniques. They expanded the crystalline unit cell manifold. Within this large unit cell the potentials are allowed to vary randomly, but periodicity is maintained between super-cells. Their justification arose from the Kohen premise of “short-sightedness” of electrons. In other words, electronic structure in solids depends predominantly on the neighborhood \mathcal{R} within the solid we are interested in. The procedure then is to construct the supercell around \mathcal{R} , incorporate the disorder within \mathcal{R} , relevant in the solid and eventually sufficiently far off impose artificial lattice translation symmetry.

The argument in support of this approach maintains that cutting off the infinite system at the supercell length scales and imposing periodic boundary conditions causes errors which cannot be worse than typical finite size effects.

Mathematically, it is the Resolvent or Green operator that carries the information of the spectrum. The Resolvent is defined as :

$$\mathbf{G}(z) = (z\mathbf{I} - \mathbf{H})^{-1}$$

z is a complex number. The spectrum of \mathbf{H} coincides with the singularities. It has poles on the real axis and the spectrum is discrete. But for manageable sized supercells the number of such poles is so large that they can mimic the continuous spectrum of the infinite system?

Let us analyze in some detail the super-cell method and its drawbacks.

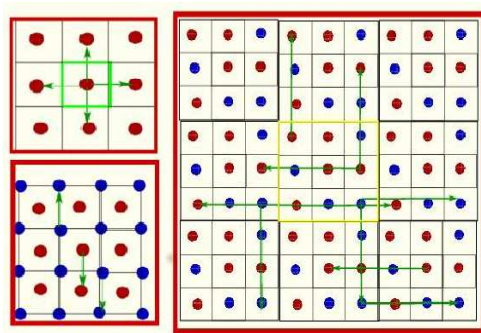


Figure 2: (Colour online) (Left panel, Top) A simple primitive cell with one atom per cell. The arrangement on the left is perfectly crystalline with lattice vectors $\{\pm a\hat{i}, \pm a\hat{j}\}$. The arrangement on the Bottom, left panel, has constructed a supercell of twice the length and breadth as the one on the left.

So there are two atoms in this unit cell. This can only be crystalline too. (Right panel) a larger super-cell with lattice vectors : $\{\pm 5a\hat{i}, \pm 5a\hat{j}\}$. Now one can introduce disorder up to this scale. Beyond this the system is again periodic.

Let us look at the Fig. 2. The top left panel shows a lattice with a primitive cell with simply one ion-core per cell, one orbital per site in the valence sea (leading to one band in the solid) and lattice vectors $\vec{\chi}_n = \pm a\hat{i} ; \pm a\hat{j}$. The ions (and hence the potential seen by the valence electrons) have perfect lattice translation symmetry and the Bloch Theorem is valid. We can therefore introduce a real, reciprocal lattice vector \vec{k} which labels both the wavefunction and the energies, which themselves are real, since the Hamiltonian is hermitian.

The wave function is :

$$\Phi_{\vec{k}}(\vec{r}, E(\vec{k})) = \exp\{i\vec{k} \cdot \vec{r}\} u_{\vec{k}}(\vec{r}, E(\vec{k})) = \langle \vec{r} | \vec{k} \rangle$$

and $u_{\vec{k}}(\vec{r} + \vec{\chi}, E) = u_{\vec{k}}(\vec{r}, E)$.

Consider a simple, tight-binding form of the Hamiltonian :

$$H = \sum_{\vec{R}} \varepsilon \mathcal{P}_{\vec{R}} + \sum_{\vec{R}} \sum_{\vec{\chi}} t(\vec{\chi}) \mathcal{T}_{\vec{R}, \vec{R} + \vec{\chi}}$$

where \mathcal{P} and \mathcal{T} are projection and transfer operators and $\vec{\chi}$ are the nearest neighbour vectors. The energy $E(\vec{k})$ is $\varepsilon + tS(\vec{k})$ where $S(\vec{k}) = \sum_{\vec{\chi}} \exp(i\vec{k} \cdot \vec{\chi})$

The resolvent of $H = (zI - H)^{-1}$ then has a representation :

$$\langle \vec{k} | (zI - H)^{-1} | \vec{k} \rangle = G(\vec{k}, z) = \frac{1}{z - E(\vec{k})}$$

The spectral function :

$$A(\vec{k}, E) = -(1/\pi) \Im \lim_{\eta \rightarrow 0} G(\vec{k}, E + i\eta) = \lim_{\eta \rightarrow 0} \frac{\eta/\pi}{[E - E(\vec{k})]^2 + \eta^2} = \delta(E - E(\vec{k})) \quad (1)$$

For a fixed value of \vec{k} this has a delta function at $E = E(\vec{k})$. If we trace out the position of the delta functions in the energy axis, we obtain the dispersion curves for the system. A part of the spectral function between the Γ and X points is shown in the left panel of Fig. 3.

Let us consider a similar case with now a larger super-cell with lattice vectors $2a \vec{i}$, $2a \vec{j}$. In this case the tight-binding Hamiltonian looks like :

$$H = \sum_{\vec{R}} \begin{pmatrix} \varepsilon_1 & \alpha \\ \alpha & \varepsilon_2 \end{pmatrix} \mathcal{P}(\vec{R}) + \sum_{\vec{R}} \sum_{\vec{\chi}} \begin{pmatrix} t(\vec{\chi}) & 0 \\ 0 & t(\vec{\chi}) \end{pmatrix} \mathcal{T}(\vec{R}, \vec{R} + \vec{\chi})$$

The two eigenvalues are now associated with site \vec{r} :

$$\mathcal{E}_n(\vec{q}) = (1/2)(E_1(\vec{q}) + E_2(\vec{q})) \pm (1/2) [(E_1(\vec{q}) - E_2(\vec{q}))^2 + 4\alpha^2]^{1/2}$$

The spectral function still remains a pair of delta functions for each value of \vec{q}

$$A(\vec{q}, E) = \sum_n \delta(E - \mathcal{E}_n(\vec{q}))$$

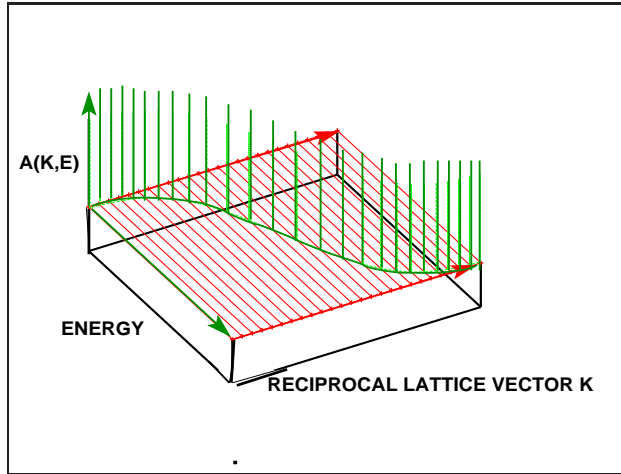


Figure 3: (Colour online) Spectral functions for \vec{k} varying between the Γ and K points : for a perfect lattice and a primitive cell containing only one atom without disorder.

The reciprocal vectors scale down to half of the original one, but because of lattice translation symmetry, the essentials of Bloch Theorem still hold. And, as long as there is lattice translation symmetry, the spectral function always remains bunches of delta functions.

$$A(\vec{q}, E) = \sum_{n=1}^N \delta(E - E_n(\vec{q}))$$

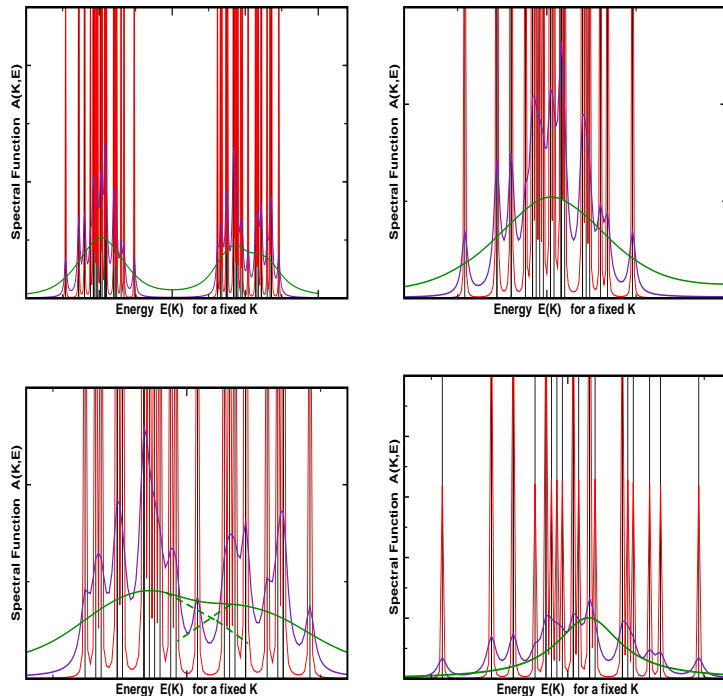


Figure 4: (Colour online) Spectral functions for different large supercells of 25 atoms. The red vertical lines mark the positions of the delta functions for a fixed \vec{q} . The indigo, blue and green curves are results of various degrees of external smoothing.

The right panel of Fig. 2 shows a super-cell with 25 lattice points and two types of atoms A and B occupying the sites occupied randomly. On the super-cell we see random configurations, but once periodic boundary conditions are imposed, the same pattern is repeated with translation vectors $5a \hat{i}$ and $5a \hat{j}$.

Note from Fig. 4 that the shape of the spectral density depends upon the exact value of the externally applied imaginary part of z . The spectral function is still a bunch of delta functions, clustered around some average energies $\ll E_n(\vec{q}) \gg$. The spectrum remains discrete and the spectral function remains a set of delta functions. The resolvent $G(\vec{k}, z)$ continues to have poles on the real z axis.

The custom then is to introduce a small complex part to z , which smoothens the spectral density :

$$A(\vec{k}, E - i\eta) = \frac{\eta/\pi}{(E - E_n(k))^2 + \eta^2}$$

and causes the “bands” to gain width^{16,17}. The complex part of z is given “by hand”, like an external parameter which, in the pure supercell method, is not obtained from first principles. The imaginary part of this complex “self-energy” which we add to z is directly related to the inverse of a disorder induced lifetime which can be measured through neutron-scattering experiments. This is one more reason we should obtain the lifetime from first principles and not from parametrization. However, if we could devise a method of mimicking the properties of the infinite sized system from those of the finite sized, but large, cell and not introduce an indeterminate parameter from outside, this approach will be on firm ground.

III. THE AUGMENTED SPACE FORMALISM

The first successful attempts at self-consistent, first-principles estimation of the “self-energy” culminated in the coherent potential approximation (CPA)^{13,14,16}. The resulting averaged resolvent maintained

all the necessary herglotz? analytic properties of the exact resolvent. The CPA was a single site formalism and any kind of multi-site correlated or uncorrelated randomness or extended defects could not be addressed by it. A majority of the earlier attempts at generalizing the CPA led to a serious debate and in 1973 Mookerjee¹⁵ proposed a way out and introduced the Augmented Space formalism¹⁷⁻¹⁹.

Suppose we have a ordered state and we measure its properties : $\mathbf{a}, \mathbf{b}, \mathbf{m}, \dots$. Absence of disorder means the measurement will give unique numbers a, b, m, \dots with probability 1. On the other hand if $\mathbf{A}, \mathbf{B}, \mathbf{M}, \dots$ are some of the disordered properties, then we cannot associate single numbers with their measurements. We have to associate a set of numbers $\{a_1, a_2, \dots\}$ and a probability density. This uncertainty may be from chemical sources or quantum mechanical. Taking cue from the latter we associate with the property an operator whose eigenvalues are the measured values and whose spectral density is the probability density of measurements.

Let us take an example Hamiltonian :

$$H = \sum_{\vec{R}} \varepsilon(\vec{R}) \mathcal{P}_{\vec{R}} + \sum_{\vec{R}} \sum_{\vec{R}+\vec{\chi}} t(\vec{\chi}) \mathcal{T}_{\vec{R}, \vec{R}+\vec{\chi}} \quad (2)$$

H is an operator in the Hilbert space \mathcal{H} spanned by the discrete basis $\{|\vec{R}\rangle\}$. Let $n_{\vec{R}}$ be a random variable which takes the values 0 and 1 with probabilities x and y ,

$$H = \sum_{\vec{R}} [\varepsilon^A n_{\vec{R}} + \varepsilon^B (1 - n_{\vec{R}})] a_{\vec{R}}^\dagger a_{\vec{R}} + \sum_{\vec{R}} \sum_{\vec{R}'} \left\{ t^{AA} n_{\vec{R}} n_{\vec{R}'} + t^{BB} [(1 - n_{\vec{R}})(1 - n_{\vec{R}'})] + \dots \right. \\ \left. t^{AB} [n_{\vec{R}}(1 - n_{\vec{R}'}) + n_{\vec{R}'}(1 - n_{\vec{R}})] \right\} a_{\vec{R}}^\dagger a_{\vec{R}'}$$

Take the rank 2 matrix $\begin{pmatrix} y & \sqrt{xy} \\ \sqrt{xy} & x \end{pmatrix}$. It has eigenvalues 0 and 1 and spectral density $x\delta(n_{\vec{R}}) + y\delta(n_{\vec{R}} - 1)$. This then fulfills our criterion discussed earlier. The matrix is a representation of an operator $\mathcal{N}_{\vec{R}}$ which acts on the 'configuration' space $\Psi_{\vec{R}}$ of rank 2 spanned by $|\alpha_{\vec{R}}\rangle = \sqrt{x}|0_{\vec{R}}\rangle + \sqrt{y}|1_{\vec{R}}\rangle$ and $|\beta_{\vec{R}}\rangle = \sqrt{y}|0_{\vec{R}}\rangle - \sqrt{x}|1_{\vec{R}}\rangle$.

$$\mathcal{N}_{\vec{R}} = y\mathcal{P}_{\alpha}^{\vec{R}} + x\mathcal{P}_{\beta}^{\vec{R}} + \sqrt{xy}\mathcal{T}_{\alpha,\beta}^{\vec{R}} \in \Psi_{\vec{R}}$$

The set of observables $\{n_{\vec{R}}\}$ is then associated with a set operators $\{\mathcal{N}_{\vec{R}}\} \in \Pi^{\otimes} \Psi_{\vec{R}}$. Thus :

$$\tilde{H} = \sum_{\vec{R}} \ll \varepsilon \gg \mathcal{P}_{\vec{R}} \otimes \mathcal{I} + \sum_{\vec{R}} (y - x)(\varepsilon^A - \varepsilon^B) \mathcal{P}_{\vec{R}} \otimes \mathcal{P}_{\beta}^{\vec{R}} + \sum_{\vec{R}} \sqrt{xy}(\varepsilon^A - \varepsilon^B) \mathcal{P}_{\vec{R}} \otimes \mathcal{T}_{\alpha\beta}^{\vec{R}} \\ + \sum_{\vec{R}} \sum_{\vec{\chi}} \left[\ll t(\vec{\chi}) \gg \mathcal{I} + (y - x)t^{(1)}(\vec{\chi})(\mathcal{P}_{\beta}^{\vec{R}} + \mathcal{P}_{\beta}^{\vec{R}+\vec{\chi}}) + \sqrt{xy} t^{(2)}(\vec{\chi})(\mathcal{T}_{\alpha\beta}^{\vec{R}} \otimes \mathcal{T}_{\alpha\beta}^{\vec{R}+\vec{\chi}}) \right] \otimes \mathcal{T}_{\vec{R}, \vec{R}+\vec{\chi}} \quad (3)$$

The augmented space theorem¹⁵ tells us :

$$\ll G(\vec{q}, z) \gg = \langle \vec{q} \otimes \emptyset | (z\tilde{I} - \tilde{H})^{-1} | \vec{q} \otimes \emptyset \rangle \quad (4)$$

where $|\emptyset\rangle = \prod^{\otimes} |\alpha_{\vec{R}}\rangle$ and $|\vec{q}\rangle = (1/N) \sum_{\vec{R}} \exp(i\vec{q} \cdot \vec{R}) |\vec{R}\rangle$. We note that if the disorder is itself homogeneous : that is the probability densities are independent of \vec{R} , then we can once again introduce an augmented reciprocal space for averaged quantities.

Our next step would be to obtain the averaged spectral function in Eqn.(4) using the recursion method proposed by Haydock and co-workers^{20,21}. We begin recursion

$$|1\rangle = |\vec{k} \otimes \emptyset\rangle \quad \tilde{H}|1\rangle = [\varepsilon + tS(\vec{k})] |1\rangle + \sqrt{xy}\Delta\varepsilon |\vec{q} \otimes \{\vec{R}\}\rangle$$

where $\{\vec{R}\}$ is the configuration $\{\alpha_1, \alpha_2 \dots \beta_{\vec{R}} \dots\}$.

$$\begin{aligned}
\alpha_1 &= \{1|\tilde{H}|1\}/\{1|1\} = \varepsilon + tS(\vec{k}) = E(\vec{q}) \\
|2\rangle &= \sqrt{xy}\Delta\varepsilon|\vec{q}\otimes\{\vec{R}\}\rangle \quad \beta_2^2 = \{2|2\}/\{1|1\} = xy(\Delta\varepsilon)^2 \\
\tilde{H}|2\rangle &= (\sqrt{xy}\Delta\varepsilon) \left\{ \varepsilon|\vec{q}\otimes\{\vec{R}\}\rangle + \sum_{\vec{\chi}} t \exp(-i\vec{q}\cdot\vec{\chi})|\vec{q}\otimes\{\vec{R}-\vec{\chi}\}\rangle + \sqrt{xy}\Delta\varepsilon|\vec{k}\otimes\emptyset\rangle \right\} \\
\alpha_2 &= \{2|\tilde{H}|2\}/\{2|2\} = \varepsilon \\
|3\rangle &= (\sqrt{xy}\Delta\varepsilon) \sum_{\vec{\chi}} t \exp(-i\vec{q}\cdot\vec{\chi})|\vec{q}\otimes\{\vec{R}-\vec{\chi}\}\rangle \\
\beta_3^2 &= Zt^2 \quad \text{where } Z \text{ is the number of nearest neighbors} \\
|N\rangle &= \tilde{H}|N-1\rangle - \alpha_{N-1}|N-1\rangle - \beta_{N-2}^2|N-2\rangle
\end{aligned} \tag{5}$$

So,

$$\{1|G(z)|1\} = G(\vec{q}, z) = \frac{1}{z - E(\vec{q}) - \frac{xy\Delta\varepsilon}{z - \varepsilon - \frac{Zt^2}{\ddots}}} = \frac{1}{g(\vec{q}, z)^{-1} - \Sigma(\vec{q}, z)}$$

where $g(\vec{q}, z) = 1/(z - E(\vec{q}))$. This leads to :

$$G(\vec{q}, z) = g(\vec{q}, z) + g(\vec{q}, z)\Sigma(\vec{q}, z)G(\vec{q}, z)$$

This is Dyson's Equation and we immediately recognize $\Sigma(\vec{q}, z)$ as the self-energy we set out to calculate.

$$\Sigma(\vec{q}, z) = \frac{\beta_2^2}{z - \alpha_2 - \frac{\beta_3^2}{z - \alpha_3 - \frac{\beta_4^2}{\ddots}}} \tag{6}$$

All practical approximations will provide us with only a finite number of $\{\alpha_n, \beta_n\}$, $n = 1, 2, \dots, N$. The question then arises that from the maximum information from the finite number of coefficients can we find the 'terminator' $T(z)$ without entering any external variable parameter.

The first information gleaned from $\{\alpha_n, \beta_n\}$, $n < N$ is the asymptotic behaviour of the coefficients. The averaged spectral function is

$$\begin{aligned}
A(\vec{k}, z) &= -\frac{1}{\pi} \Im m \ll G(\vec{k}, z) \gg \\
&= \frac{\Sigma_{im}(\vec{k}, z)/\pi}{(g^{-1}(\vec{k}, z) - \Sigma_{real}(\vec{k}, z))^2 + (\Sigma_{im}(\vec{k}, z))^2}
\end{aligned} \tag{7}$$

This $\Sigma_{im}(\vec{k}, z) = 1/\tau$ is the disorder induced lifetime²² of a \vec{k} labeled quantum state.

IV. APPLICATION TO DOPED GRAPHENE

Here we have used random vacancies as defect in graphene sheet. For a random representation of carbon with vacancies the Hamiltonian was derived self-consistently from the DFT self-consistent tight-binding linear muffin-tin orbitals augmented space recursion (TB-LMTO-ASR) package developed by our group²³. In the next step, Nth Order Muffin Tin Orbital (NMTO) method was used to construct the low-energy Hamiltonian. All the calculations are done at T=0 K.

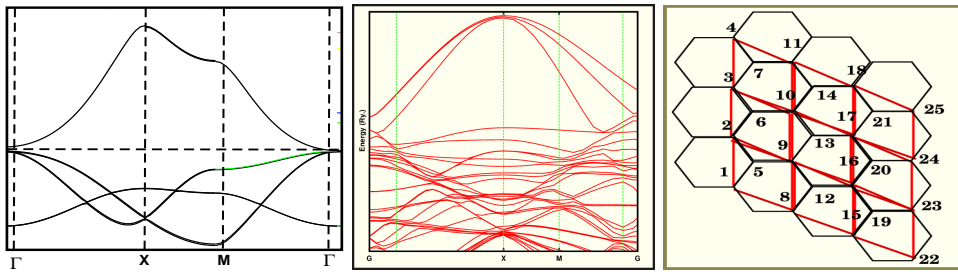


Figure 5: (Left) The dispersion relation for pristine graphene. (Middle) The unsmoothed averaged dispersion relation for graphene with 5% random vacancies. This has been calculated from a super cell made out of nine original unit cells, as shown in the panel on the right.

(eV)	ε	$t(\chi_1)$	$t(\chi_2)$	$t(\chi_3)$
	-0.291	-2.544	0.1668	-0.1586

Table I: Tight-binding parameters of Hamiltonian generated by NMT0. χ_n refer to the n-th nearest neighbor vector on the lattice.

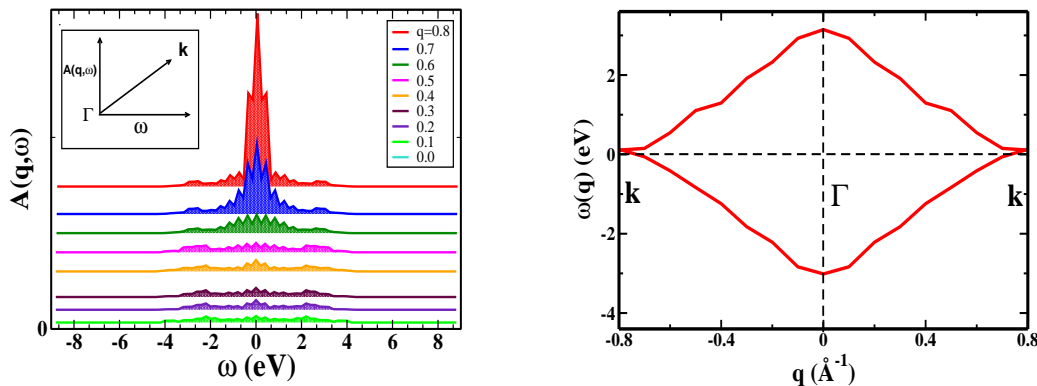


Figure 6: (Colour online)(left) Spectral functions $A(\vec{q}, \omega)$ for \vec{q} varying between the Γ and K points for a Graphene lattice with 5% vacancy content. (right) The band dispersion near the Fermi level in the first Brillouin zone graphene with 5% vacancy concentration obtained by following the peak-finding process of spectral function of $A(\vec{q}, \omega)$ described in the text. The Fermi level is at 0 eV. The linear dispersion at K point is slightly shifted upwards from Fermi level due to disorder.

We have used augmented block recursion technique to study the energy band dispersion of doped Graphene. We have calculated the spectral function $A(\vec{q}, \omega)$ as shown in Fig (6) for a selection of different wave vectors q varying from 0.0 to 0.8 along the symmetric $\Gamma - K$ with 5% vacancy concentration. The spectral intensity of $A(\vec{q}, \omega)$ is low at $q = 0.0 \text{ \AA}^{-1}$ ie at Γ point , and increases with increasing the wave vector q . This is made clear by observing the peaks located at $q = 0.0 \text{ \AA}^{-1}$ and 0.8 \AA^{-1} . The spectral intensity $A(\vec{q}, \omega)$ is getting highest at dirac point ie at K point. These peak positions are shifted to lower energies with increasing wave vector q captured by our method. The peak width get broden with increasing wave vector q . We obtain the band dispersions by identifying the peak positions of the spectral function $A(\vec{q}, \omega)$ along high symmetric directions in reciprocal space²⁴⁻²⁷ for doped graphene. The calculated dispersion of the $\pi - \pi^*$ bands is displayed in Fig 6 for doped graphene with 5% vacancy concentration. Doped graphene shows linear dispersion relation above the Fermi level. The p_z branches of graphene shows the typical cusp like behavior at the K point leading to its ‘semi-metallic’ behavior. Band dispersion (BD) of disordered graphene shows linear dispersion only at K points above the Fermi level. For such a sp^2 bonded structure, the σ bond is responsible for the formation of the underlying framework. The remaining p_z orbital , which is roughly vertical to the tetra or hexa-rings, binds covalently with each

other and forms π and π^* bands. These π and π^* are believed to induce the linear dispersion relation near the Fermi surface. Experimentally it is observed that Silicene has a similar BS and Dirac-like fermions with regular hexagonal symmetry²⁸⁻²⁹.

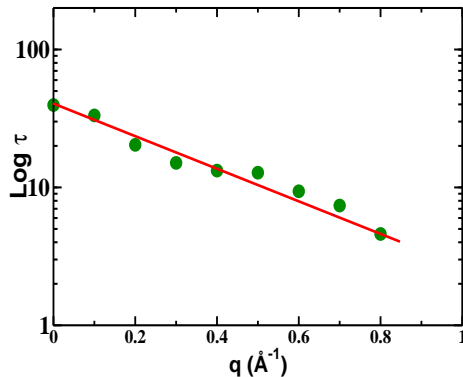


Figure 7: (Colour online) Relaxation time of graphene for \vec{q} varying between the Γ and k points with 5% vacancy content from disordered induced self energy Σ_{e-e} .

Disordered (vacancy induced) graphene leads to two distinct momentum relaxation times ; the transport relaxation time and the quantum lifetime or the single-particle relaxation time. Our recent study does not take into account the transport relaxation time, we only calculate the single-particle relaxation time $\tau(\vec{q})$. From a many-body-theory viewpoint the single particle relaxation time $\tau(\vec{q})$ is calculated from the electron self energy of the coupled electron-impurity system. We obtain disorder induced lifetime τ of a \vec{q} labeled quantum state from the Fourier transform of the configuration averaged self energy function. Finally, in Fig. 7 we show our calculated single particle relaxation time $\tau(\vec{q})$ as a function of q (\AA^{-1}) in 1st Brillouin Zone for graphene. The relaxing modes or patterns are labeled by q , such that the average 'size' of the mode is $O(q^{-1})$. We define the lifetime $\tau(\vec{q})$ as the time in which the disordered induced self energy amplitude drops to its $1/e$ value. The central impurity peak is increasing with increasing vacancy (disorder) content. We note that $\text{Log } \tau(\vec{q})$ decreases almost linearly with increasing wave vector q . To date, most experimental studies have focused on the transport scattering time. Both the single particle relaxation time and transport scattering time are important for carrier mobilities (μ) of 2D graphene like systems . This two types of scattering time ratio is needed for describing scattering mechanism in such 2D systems. It is important to note that the single particle relaxation time $\tau(\vec{q})$ is accessible to neutron scattering experiments.

V. CONCLUSION

In conclusion, we present a theoretical method to study the effects of disorder in describing the spectral properties of graphene within the framework of Green function. We show how the topology of the Dirac dispersion, and the location of Dirac point change with disorder. We also obtain disorder induced lifetime without external parameter fitting in the complex part of energy. The single particle relaxation time $\tau(\vec{q})$ has been obtained from the broadening of quantum states due to disorder. Disorder-induced broadening, related to the scattering length (or life-time) of Bloch electrons. We believe that such a study may provide a useful insight into the scattering mechanism of doped graphene. Finally, we believe that our framework is suitable for the study of the effects of disorder in other 2D materials such as Silicene, boron nitride mono layer.

ACKNOWLEDGEMENTS

The authors would like to thank Dhani Nafday and Tanusri Saha-Dasgupta for providing us with the Hamiltonian parameters calculated by NMTO code. We would like to thank Prof. O.K. Anderson, Max

Plank Institute, Stuttgart, Germany, for his kind permission to use TB-LMTO code developed by his group.

-
- ¹ Bloch, F. , Z. Physik **52** 555 (1928).
² Hohenberg, P. and Kohn, W., Phys. Rev. **136** B864 (1964)
³ Kohn, W. and Sham, L.J., Phys. Rev. **140** A1133 (1965)
⁴ Floquet, G., Annales de l'École Normale Supérieure **12** 47 (1883)
⁵ Hill, G.W., Acta Math. **8** 1 (1886).
⁶ Fóll, H. in "Periodic Potentials and Bloch's Theorem – lectures in "Semiconductors I", The University of Kiel (1976)
⁷ Eastham, M.S.P. , in "The Spectral Theory of Periodic Differential Equations." Edinburgh: Scottish Academic Press (1973).
⁸ Lyapunov, A.M. , in "The General Problem of the Stability of Motion." London: Taylor and Francis.(1992)
 Translated by A. T. Fuller from Edouard Davaux's French translation (1907) of the original Russian dissertation (1892).
⁹ Anderson, P.W. , Phys. Rev. **109** 1492 (1958)
¹⁰ Kumar, N. and Jayannavar, A. , Phys. Rev. Lett. **48** 553 (1982)
¹¹ Tit, N., Pradhan, P. and Kumar, N., Phys. Rev. **B49** 14715 (1994)
¹² Mott, Sir N. in "Conductance in Non-Crystalline Materials" (Clarendon Press) (1986)
¹³ Soven, P., Phys. Rev. **156** 809 (1967)
¹⁴ Kopernik, K. , Eschrig, H., Velický, B. and Hayn, R., Phys. Rev. **B55** (1997)
¹⁵ Mookerjee, A., J. Phys. C : Solid State Phys **6** 1340 (1973)
¹⁶ Mookerjee, A., J. Phys. C : Solid State Phys **8** 29 (1975)
¹⁷ Mookerjee, A., J. Phys. C : Solid State Phys **8** 1524 (1975)
¹⁸ Mookerjee, A., J. Phys. C : Solid State Phys **8** 2688 (1975)
¹⁹ Mookerjee, A., J. Phys. C : Solid State Phys **8** 2943 (1975)
²⁰ Haydock, R. , Heine, V. and Kelly, M.J., J. Phys. C: Solid State Phys **5** (1972) 2845.
²¹ Haydock, R. in "Solid State Physics", edited by H. Ehrenreich, F. Sietz, D. Turnbull, Academic, New York, 35 (1980).
²² S. Doniach, E. H. Sondheimer *Green's Functions for Solid State Physicists* Imperial College Press, (1998), chapter-V,137
²³ A . Mookerjee, in A . Mookerjee, D.D Sarma (Eds.), *Electronics Structure of Clustures, Surfaces and Disordered Solids*, Taylors Francis , 2003
²⁴ B. Skubic, J. Hellsvik, L. Nordström, and O. Eriksson, *J. Phys.Condens.Matter* **20**, 31 (2008)
²⁵ X.Tao, D.P.Landau, T.C.Schulthess, and G.M.Stocks, *Phys.Rev. Lett.* **95**, 087207 (2005)
²⁶ K. Chen and D. P. Landau, *Phys. Rev.B* **49**, 3266 (1994)
²⁷ Anders Bergman, Andrea Taroni, Lars Bergqvist, Johan Hellsvik, Björgvin Hjörvarsson, and Olle Eriksson *Phys. Rev.B* **81**, 144416 (2010) DOI: 10.1103/PhysRevB.81.144416
²⁸ S. Cahangirov, M. Topsakal, E. Aktuik, H. Sahin, and S. Ciraci, *Phys. Rev. Lett.* **102**, 236804 (2009).
²⁹ P. De Padova, C. Quaresima, C. Ottaviani, P. M. Sheverdyaeva, P. Moras, C. Carbone, D. Topwal, B. Olivieri, A. Kara, H. Oughaddou, B. Aufray, and G. Le